



HAL
open science

Dielectric relaxation and localized electron hopping in colossal dielectric (Nb,In)-doped TiO₂ rutile nanoceramics

Kosuke Tsuji, Hyuksu Han, Sophie Guillemet Fritsch, Clive A. Randall

► **To cite this version:**

Kosuke Tsuji, Hyuksu Han, Sophie Guillemet Fritsch, Clive A. Randall. Dielectric relaxation and localized electron hopping in colossal dielectric (Nb,In)-doped TiO₂ rutile nanoceramics. *Physical Chemistry Chemical Physics*, 2017, 19 (12), pp.8568-8574. 10.1039/C7CP00042A . hal-02401486

HAL Id: hal-02401486

<https://hal.science/hal-02401486>

Submitted on 10 Dec 2019

HAL is a multi-disciplinary open access archive for the deposit and dissemination of scientific research documents, whether they are published or not. The documents may come from teaching and research institutions in France or abroad, or from public or private research centers.

L'archive ouverte pluridisciplinaire **HAL**, est destinée au dépôt et à la diffusion de documents scientifiques de niveau recherche, publiés ou non, émanant des établissements d'enseignement et de recherche français ou étrangers, des laboratoires publics ou privés.



Open Archive Toulouse Archive Ouverte (OATAO)

OATAO is an open access repository that collects the work of Toulouse researchers and makes it freely available over the web where possible

This is an author's version published in: <http://oatao.univ-toulouse.fr/24484>

Official URL: <https://doi.org/10.1039/C7CP00042A>

To cite this version:

Tsuji, Kosuke and Han, Hyuksu  and Guillemet, Sophie  and Randall, Clive A. *Dielectric relaxation and localized electron hopping in colossal dielectric (Nb,In)-doped TiO₂ rutile nanoceramics*. (2017) *Physical Chemistry Chemical Physics*, 19 (12). 8568-8574. ISSN 1463-9076

Any correspondence concerning this service should be sent to the repository administrator: tech-oatao@listes-diff.inp-toulouse.fr

Dielectric relaxation and localized electron hopping in colossal dielectric (Nb,In)-doped TiO₂ rutile nanoceramics

Kosuke Tsuji,^a HyukSu Han,^{bc} Sophie Guillemet Fritsch^c and Clive A. Randall^{*a}

Dielectric spectroscopy was performed on a Nb and In co-doped rutile TiO₂ nano-crystalline ceramic (n-NITO) synthesized by a low-temperature spark plasma sintering (SPS) technique. The dielectric properties of the n-NITO were not largely affected by the metal electrode contacts. Huge dielectric relaxation was observed at a very low temperature below 35 K. Both the activation energy and relaxation time suggested that the electronic hopping motion is the underlying mechanism responsible for the colossal dielectric permittivity (CP) and its relaxation, instead of the internal barrier layer effect or a dipolar relaxation. With Havriliak-Negami (H-N) fitting, a relaxation time with a large distribution of dielectric relaxations was revealed. The broad distributed relaxation phenomena indicated that Nb and In were involved, controlling the dielectric relaxation by modifying the polarization mechanism and localized states. The associated distribution function is calculated and presented. The frequency-dependent a.c. conductance is successfully explained by a hopping conduction model of the localized electrons with the distribution function. It is demonstrated that the dielectric relaxation is strongly correlated with the hopping electrons in the localized states. The CP in SPS n-NITO is then ascribed to a hopping polarization.

DOI: 10.1039/c7cp00042a

Introduction

It is of interest to search for colossal permittivity (CP) materials for low-frequency capacitor applications. In the last 20 years or so, CP has been reported in many material systems, such as CaCuTiO₁₂,^{1,2} doped-NiO,³ Ba₄YMn₃O_{11.5},⁴ and CuO.⁵ The CP in these materials has been explained in terms of Maxwell-Wagner interfacial polarization, resulting from a depletion layer between grain/grain boundary or grain/electrode interfaces. The former case is often referred to as “internal barrier layer capacitance (IBLC)”. The CP owing to Maxwell-Wagner polarization, however, is often accompanied by a high dielectric loss ($\tan \delta > 0.05$) and temperature-frequency instabilities.⁶

In 2013, Hu *et al.* demonstrated that a (Nb,In)-doped TiO₂ (NITO) rutile structure could achieve CP ($\sim 6 \times 10^4$) with $\tan \delta < 0.05$ and excellent temperature-frequency characteristics over 100–400 K and 10–10⁵ Hz.⁷ Yet the origin of the mechanism of the dielectric properties is not fully clarified. They correctly assumed a complex and localized defect dipole relaxation, and

this was inferred from a combination of density functional theory calculations, as well as structural and electrical characterizations. Later, their conclusions were further supported by other groups.^{8–10} In contrast, the IBLC effect has also been proposed as an origin of CP in NITO ceramics. The resistive grain boundaries in NITO ceramics were elucidated by current-voltage and impedance measurements.^{11–13} More recently, some alternative explanations, such as polaronic relaxation,¹⁴ or a mixed contribution of the defect-dipole, polaronic, and electrode-ceramic interface effect, have been proposed.¹⁵ In many cases, the origin of CP has been argued by the existence of the “barrier”, that is, the resistance and activation energy of the grain and grain boundaries. But complexities arise from the fact that the IBLC effect could have less significance, even though the barrier layer structure exists in one material.^{16,17}

In early research on the dielectric relaxation phenomenon, Debye showed that a complex permittivity, ϵ^* , would have a functional form of¹⁸

$$\epsilon^*(\omega) = \epsilon_{\infty} + \frac{\epsilon_s - \epsilon_{\infty}}{1 + j\omega\tau} \quad (1)$$

where ϵ_s and ϵ_{∞} are the static and dynamic permittivity values. ω and τ are the angular frequency and relaxation time, respectively. Although τ is known to have a characteristic time depending on the relaxation mechanism, less attention has been paid to the argument for CP in NITO compared to the barrier layer

^a Center for Dielectrics and Piezoelectrics, Materials Research Institute, Department of Material Science and Engineering, The Pennsylvania State University, University Park, Pennsylvania 16802, USA. E-mail: car4@psu.edu

^b Korea Institute of Industrial Technology, Gwahakdanji-ro 137-41, Gangwon-do, 25440, Republic of Korea

^c CIRIMAT, Université de Toulouse, CNRS, UPS, INP, 118 route de Narbonne, 31062, Toulouse Cedex 9, France

characteristics. Therefore, an extensive study on the relaxation phenomena with a classical theoretical work, such as Havriliak–Negami,¹⁹ Jonscher,²⁰ or Macdonald,²¹ should give critical insights into the physical aspects of the CP in NITO ceramics.

Previously, we demonstrated that the CP in nano-crystalline NITO (n-NITO) ceramics synthesized by a low-temperature spark plasma sintering (SPS) technique is not owing to the IBLC effects and is ascribed to the relaxation of localized electrons.²² In the present work, we investigate the dielectric relaxation, focusing on the origin of CP in n-NITO ceramics. First, the electrode–ceramic interface effect was investigated. Then, dielectric spectroscopy was performed on a huge dielectric relaxation in n-NITO. The nature of the relaxation is discussed based on the Havriliak–Negami (H–N) model. The role of the localized electrons for the CP is explained through the correlation with the a.c. transport mechanism.

Experimental

NITO powders were prepared by the oxalate precipitation method used in a previous work.²² Raw powders, InCl₃ (Sigma-Aldrich, 98%) and NbCl₅ (Sigma-Aldrich, 99%), were all dissolved in water and ethanol and then mixed with a lab made TiOCl₂ oxalic acid solution. Then, oxalic acid was added to the final precursors and homogeneous oxalates were precipitated. The precipitate was dried at 120 °C overnight and calcined at 1000 °C for 1 hour under static air. The oxide powder was then sintered using a Dr Sinter 2080 SPS system (Sumitomo Coal Mining Co., Tokyo, Japan). SPS conditions were maintained at 800 °C under 100 MPa for 20 minutes. As-sintered specimens underwent post-annealing at 600 °C for 12 hours in static air. More processing details are described in ref. 22. Au and Pt electrodes (99.99%, Kurt J. Lesker Company, USA) were coated by a sputter coater (EMS 150 R S, Electron Microscopy Sciences, USA). Ag electrodes were painted on and dried in air. Impedance measurement was performed using a computer-controlled LCR meter (HP 4284A, Hewlett-Packard, USA).

Results and discussion

Fig. 1(a) shows the frequency dependence of the dielectric properties of n-NITO ceramics with different metal electrodes at room temperature. Both ϵ' and $\tan \delta$ are almost invariant to the kind of electrode. The slight difference with the electrode metal in this work is much smaller than the reported electrode–ceramic interface effect in Nb + Ga co-doped rutile TiO₂, which showed an order of magnitude difference.¹⁵ The relaxation in ϵ' and $\tan \delta$ above 350 K shown in Fig. 1(b) may be caused by this electrode–ceramic interface. Similar observations are also reported in NITO and other ceramics.^{14,23} It is often caused by charge accumulation at an interface due to the delocalized electron at high temperatures. Then, the relaxation at the higher temperature could be associated with the electrode/sample effect, but it is unlikely that it is the origin of the large permittivity ($\epsilon' \sim 5000$) below room temperature. Fig. 1(b) shows that the dielectric properties possess a stable temperature-independent characteristic at lower temperatures.

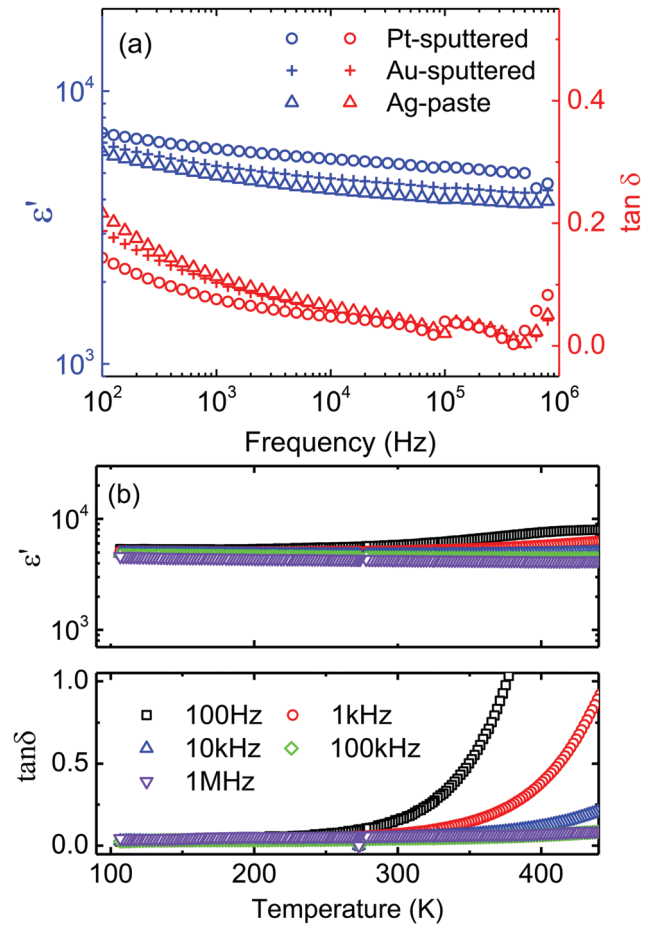


Fig. 1 Dielectric properties of n-NITO (a) as a function of frequency with Pt, Au and Ag electrodes at room temperature, and (b) as a function of temperature with an Au electrode.

As shown in Fig. 2(a), ϵ' started to rapidly decrease below 35 K from the higher frequency side, though the plateau regime of ϵ' could not be observed, due to the measurement limit ($f < 2 \times 10^6$ Hz). It is clear that the relaxation in Fig. 2(a), which should be caused by one polarization mechanism, achieved CP above 35 K in n-NITO ceramics. Meanwhile, the imaginary part of the relative permittivity, ϵ'' , shows a Debye-like relaxation peak. As temperature decreased, the loss peak in ϵ'' shifted towards lower frequency, with a slight increase of the peak height. For this kind of a thermally-activated process, the relaxation time, τ , in eqn (1) is given by the Arrhenius law:²⁴

$$\tau = 1/\omega_r = 1/2\pi f_r = \tau_0 \exp\left(\frac{E_a}{k_B T}\right) \quad (2)$$

where E_a , k_B , T , τ_0 and $f_r(=\omega_r/2\pi)$ are the activation energy, the Boltzmann constant, the temperature, the pre-exponential factor, and the frequency at the peak maximum, respectively. The f_r was obtained from the frequency at the peak maximum of ϵ'' , as shown in Fig. 2(a). An Arrhenius plot of eqn (2) is shown in Fig. 2(b), where $E_a = 9.33 \times 10^{-3}$ eV and $\tau_0 = 1.44 \times 10^{-9}$ s were provided respectively. Table 1 summarizes τ_0 and E_a for various types of relaxation in some ceramics. The typical E_a for

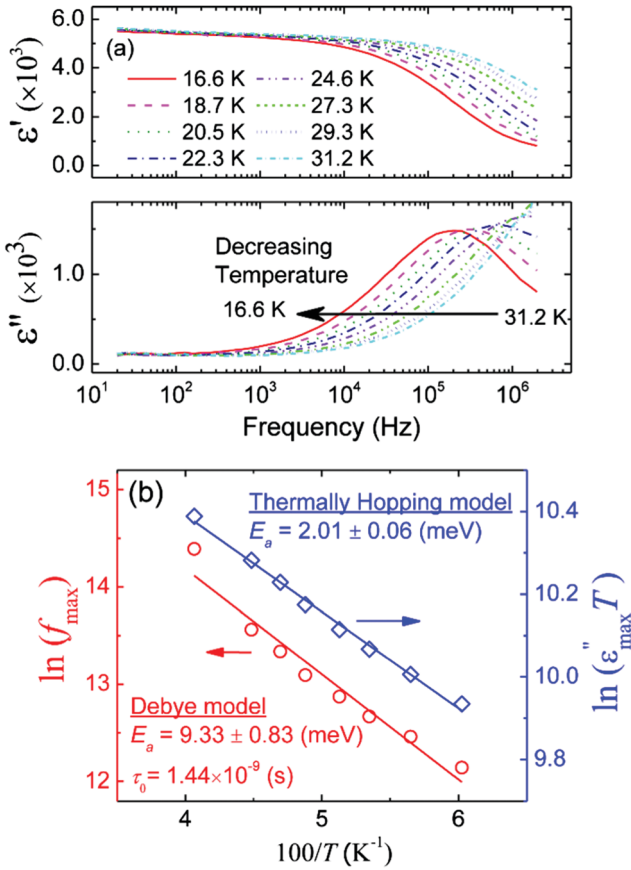


Fig. 2 (a) Frequency dependence of ϵ' and ϵ'' in n NITO at different temperatures ($T = 16.6$ – 31.2 K), and (b) the Arrhenius plot of the Debye model (eqn (2)) and the thermally activated hopping model (eqn (3)).

both the Maxwell-Wagner and dipolar relaxations requires much larger E_a to describe either an interfacial potential barrier at the grain boundaries²⁵ or an ionic motion over the local potential well.^{26,27} As a result, relaxations corresponding to either of those mechanisms are observed at higher temperatures ($T > \text{R.T.}$) due to the large value of E_a .^{1,28–31} Thus, these types of relaxations are both ruled out as an origin of the large relaxation in Fig. 2. Instead, the smaller value of E_a suggests that the relaxation may originate from a localized electronic motion.

The measured $E_a = 9.33 \times 10^{-3}$ eV and $\tau_0 = 1.44 \times 10^{-9}$ s are close to typical polaronic relaxations in many material systems, as shown in Table 1. Thus, hopping and trapped electrons are believed to cause the relaxation phenomena.³² The electron hopping between two cation sites corresponds to a redistribution of charge and creation of a local dipole, and this can result in a large permittivity. One can find from eqn (2) that the smaller values of E_a and τ_0 should result in a fast relaxation process at a fixed temperature, so that the hopping type of relaxations have been observed at low temperature ($T < 100$ K) with a frequency range of less than 10^6 Hz.^{33–36} In our case, the characteristic time constant τ exponentially became faster (smaller) as the temperature increased, and then it reached $\tau \sim 6 \times 10^{-8}$ s at 30 K, which corresponds to $f_r > 2 \times 10^6$ Hz. Hence, relaxation was not clearly observed in the measured frequency range above 30 K in Fig. 2(a). The temperature–frequency stable characteristics of ϵ' in Fig. 1 are then attributed to the small values of τ_0 and E_a by increasing the f_r out of the measurement frequency range ($f_r > 10^6$ Hz). Also, our result, $E_a = 9.33 \times 10^{-3}$ eV and $\tau_0 = 1.44 \times 10^{-9}$ s, predicts that the dispersion appears at $f_r \sim 7 \times 10^7$ Hz at 298 K, which is consistent with the frequency-independent large permittivity of amorphous NITO thin film up to 10^7 Hz.⁸ For practical applications, the utilization of hopping polarization with the smaller values of E_a and τ_0 should have an advantage for the more stable temperature–frequency characteristics in a capacitor application. Our previous report demonstrated that the fast and low temperature processing by SPS may have been helpful to achieve such novel characteristics by suppressing the IBLC effect.²² When the hopping polarization is involved, the peak maximum of the loss peak can be represented by³⁷

$$T \epsilon_{\text{max}}'' = \frac{N_0 \mu^2}{3k_B} \exp\left(\frac{E_a}{k_B T}\right) \quad (3)$$

where μ and N_0 are the local dipole moment and the pre-exponential factor of the hopping dipole. ϵ_{max}'' is the loss peak maximum at various temperatures obtained from Fig. 2(a). The Arrhenius form of eqn (3) is then plotted in Fig. 2(b). As can be seen, the experimental data follow eqn (3). The $E_a = 2.01 \times 10^{-3}$ eV value was found to be relatively smaller than the $E_a = 9.33 \times 10^{-3}$ eV value from eqn (2), but the same order is maintained. Then, the

Table 1 Summary of relaxation parameters for different mechanisms

Material	E_a (eV)	τ_0 (s)	Mechanism	Ref.
CaCu ₃ Ti ₄ O ₁₂	0.60	7×10^{14}	Maxwell Wagner	1
TiO ₂	0.70	2×10^{11}	Maxwell Wagner	28
Mg doped BaTiO ₃	0.46–0.53	^a	Dipolar (Mg_{Ti}'' $\text{V}_{\text{O}}^{\bullet\bullet}$)	29
Zr doped SrTiO ₃	0.77–0.86	^a	Dipolar (V_{Sr}'' $\text{V}_{\text{O}}^{\bullet\bullet}$)	30
NiO	0.30	1.6×10^6	Dipolar (Ni'_{Ni} $\text{V}_{\text{Ni}}^{\bullet\bullet}$)	31
SrTi _{1-x} (Mg _{1/3} Nb _{2/3}) _x O ₃	0.005	$(1.4–1.7) \times 10^9$	Polaronic	33
SrTiO ₃ –SrMg _{1/3} Nb _{2/3} O ₃	0.001	10^{10} – 10^8	Polaronic	34
Pt _{1-x} Ca _x MnO ₃	0.04–0.14	10^{11} – 2.5×10^9	Polaronic	35
TiO _{2-x}	0.02	10^7 – 10^8	Polaronic	36

^a Not given in the references.

electron hopping model in n-NiTO is therefore further suggested in this system. The small discrepancy is discussed in a later section.

Fig. 3(a) shows a complex permittivity ε^* plot of n-NiTO at 16.6 K. Clearly, the “suppressed” semi-circle of $\varepsilon^*(\omega)$ suggests the deviation from the Debye relaxation. The $\varepsilon^*(\omega)$ value in eqn (1) can be expressed using a more general form, known as the Havriliak–Negami (H–N) relaxation:¹⁹

$$\varepsilon^*(\omega) = \varepsilon_\infty + \frac{\varepsilon_s - \varepsilon_\infty}{(1 + (j\omega\tau_{\text{HN}})^\alpha)^\beta} \quad (4)$$

Eqn (4) is reduced to eqn (1) when $\alpha = \beta = 1$. Also, $\alpha = 1, 0 < \beta < 1$ is referred to as the Cole–Davidson equation. α is the parameter for the peak breadth of the distribution and β is the parameter for the symmetry of the distributed function. Fig. 3(a) shows the fitting results with the H–N model and the Debye model ($\alpha = \beta = 1$). The best fit was given with the exponents; $\alpha = 0.63, \beta = 0.99$, and the characteristic time constant $\tau_{\text{HN}} = 8.9 \times 10^{-7}$ s, respectively. Such a low value of α indicates that the relaxation time is widely distributed, but with a symmetrical distribution ($\beta = 0.99$). The observed relaxation should then be explained by the Debye-like”

relaxation with the distribution function. The distribution function is given as follows:^{19,38}

$$F(\tau/\tau_{\text{HN}}) = \left(\frac{1}{\pi}\right) (\tau/\tau_{\text{HN}})^{\alpha\beta} \sin(\beta\theta) \left((\tau/\tau_{\text{HN}})^{2\alpha} + (\tau/\tau_{\text{HN}})^\alpha + 1 \right)^{-\beta/2} \quad (5)$$

with

$$\theta = \arctan\{\phi\} \quad (\phi > 0) \quad (6)$$

$$\theta = \arctan\{\phi\} + \pi \quad (\phi < 0)$$

$$\phi = \frac{(\omega\tau_{\text{HN}})^\alpha \sin(\pi\alpha)}{(\tau/\tau_{\text{HN}})^\alpha + \cos(\pi\alpha)} \quad (7)$$

Fig. 3(b) shows $F(\tau/\tau_{\text{HN}})$ at 16.6 K in n-NiTO ceramics calculated with $\alpha = 0.63, \beta = 0.99$ and $\tau_{\text{HN}} = 8.9 \times 10^{-7}$. As expected, $F(\tau/\tau_{\text{HN}})$ is nearly symmetric and widely distributed over decades. The distributed τ is often ascribed to a distribution of activation energy.^{39,40} In this case, we believe that it originates from localized states interacting with the surrounding ions, as suggested for polaronic hopping.⁴¹ The multiple Debye-type relaxations with distributed E_a overlap each other and show a broad distribution of τ .²⁰ It is suggested that dielectric relaxations in Fig. 2(a) and 3 are associated with the electron hopping among the distributed potential wells. The total time for the electron to move and for the surrounding atoms to reach the thermal equilibrium positions may vary with each localized state. Then, the dopant should also play an important role in increasing the number of the local dipoles, N . Nb-doping increased the carrier concentration and the number of Ti'_{Ti} sites. The increased number of hopping electrons should enhance the N value, contributing to the net polarization. In fact, it was reported that Nb-only doped TiO_2 could show a large permittivity ($\varepsilon' > 10^4$) with $\tan \delta > 0.1$, while In-only doped TiO_2 produced $\varepsilon' \sim 120$.⁷ Since Nb and In co-doped TiO_2 showed a lower loss ($\tan \delta < 0.1$), In-doping may influence the localized states of electrons. The hopping model proposed in this work may not contradict the defect cluster model.⁷ Maglione *et al.* suggested that the electron relaxation could occur in the defect cluster at low temperatures.⁴² Further work is needed to better understand how the defects are involved with the relaxation.

Unfortunately, the good fitting results with eqn (4) could not be obtained above $T > 22$ K, due to the lack of a higher frequency part of ε'' . However, the relationship $\ln(\tau_{\text{HN}})$ vs. $1/T$ in the small temperature range yielded similar results to Fig. 2 and eqn (2) ($E_a = 6.8 \times 10^{-3}$ eV and $\tau_0 = 7.9 \times 10^{-9}$ s). This is probably because $F(\tau/\tau_{\text{HN}})$ was nearly symmetrical, so it did not affect the position of the loss peak. Thus, we believe that the previous result of τ_0 and E_a shown in Fig. 2 should be valid. Fig. 4 shows the normalized loss peak from Fig. 2(a). The peak shape is almost invariant with temperature. In addition, the slope of the left side of the loss peak at even higher temperatures up to 31.2 K in Fig. 2(a) was also invariant with temperature change ($s \sim 0.48 \pm 0.02$ in $\varepsilon'' \sim \omega^s$). Thus, α, β and hence the distribution function were probably not very sensitive to temperature in the measured temperature range. Similar observations have been reported.^{43,44} Therefore, similar $F(\tau/\tau_{\text{HN}})$ is expected in the measured temperature range in Fig. 2.

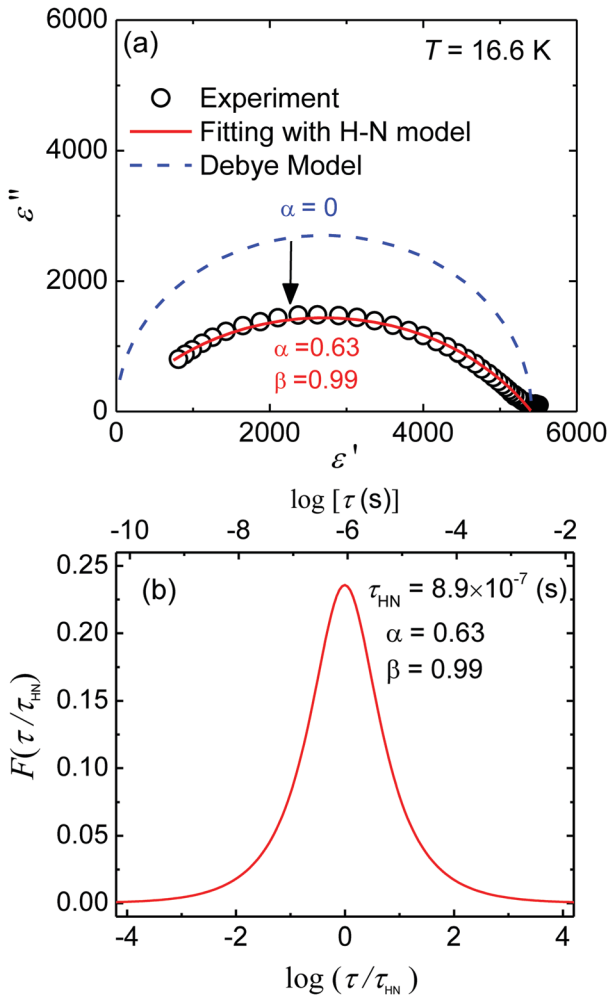


Fig. 3 (a) The ε^* plot of n NiTO fitted with the Debye model and the Havriliak–Negami (H–N) model, and (b) the calculated distribution function, $F(\tau/\tau_{\text{HN}})$, at 16.6 K. The FWHM was found to be ~ 1.45 .

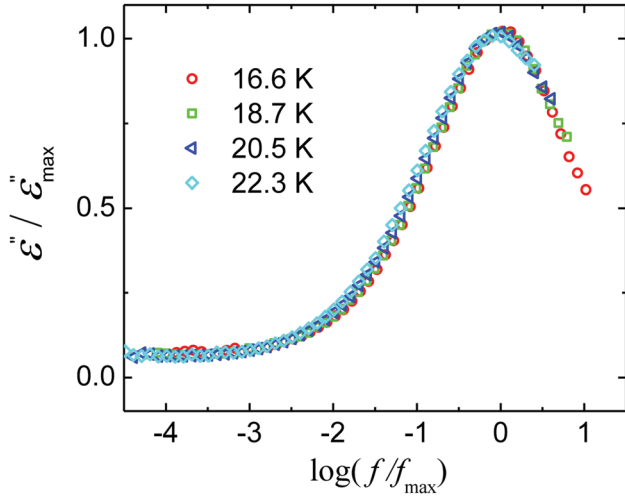


Fig. 4 Normalized ε'' of permittivity in n-NiTO at different temperatures.

For the hopping electrons, frequency-dependent a.c. conductivity is expected.²¹ In the case of a constant activation energy profile, the a.c. conductivity is expected to be constant as a function of the frequency and determined by the barrier height between two states (Fig. 5(a)). In the double potential well, the a.c. conductivity tends to be zero at lower frequencies because of the infinite potential. The conductivity then increases at higher frequencies because of the Debye-like transition in Fig. 5(b). The theory for this type of hopping conduction had been proposed as follows:^{32,45,46}

$$\sigma'(\omega) = \frac{A}{kT} \exp\left(-\frac{E'}{kT}\right) \frac{\omega^2 \tau}{1 + (\omega\tau)^2} \quad (8)$$

where A , E' and τ_0 are the constants for the hopping, the energy difference separating two sites and the characteristic relaxation

time. Here, τ should be close to τ_{HN} . One can find that eqn (8) has a form of $\sigma'(\omega) \sim \omega \varepsilon''(\omega)$ with a Debye loss term, $(\omega\tau/1 + (\omega\tau)^2)$. Then eqn (8) predicts $\sigma'(\omega) \propto \omega^2$ at $\omega < \omega_r$ and $\sigma'(\omega) = \text{const.}$ at $\omega_r < \omega$ at fixed temperature as shown Fig. 5(b). In the case of the multiple activation energies, a combination of the Debye-like transition gives rise to the step-like profile corresponding to each activation energy (Fig. 5(c)). Fig. 6 shows the frequency dependence of the a.c. conductance, $Y(\omega)$, of n-NiTO ceramics as a function of temperature. The $Y(\omega)$ value greatly increased with the increase of f . The slope, s , is found to be $s \sim 1.47$ at $f \sim 10^4$ Hz and $s \sim 0.63$ at the higher frequency side of f_r with a slight temperature dependence. The frequency dependence of the experimental data, $s \sim 1.47$, in Fig. 6 cannot be explained by the simple hopping model in Fig. 5(a)–(c). This is because the activation energies in n-NiTO are expected to be widely distributed as suggested by the H–N fitting. As shown in Fig. 5(d) and (e), such widely distributed potential wells would give rise to the smooth profile in the a.c. conductivity by overlapping the step-like profile. Thus, $Y(\omega)$ at 16.6 K was fitted including distribution parameters. The H–N model gives $\varepsilon''(\omega)$ in the following form:¹⁹

$$\varepsilon''(\omega) = (\varepsilon_s - \varepsilon_\infty) r^{-\beta/2} \sin \beta\theta \quad (9)$$

with

$$r = \left\{ 1 + (\omega\tau)^z \sin\left(\frac{\alpha\pi}{2}\right) \right\}^2 + \left\{ (\omega\tau)^z \cos\left(\frac{\alpha\pi}{2}\right) \right\}^2 \quad (10)$$

$$\theta = \arctan \left\{ \frac{(\omega\tau)^z \cos\left(\frac{\alpha\pi}{2}\right)}{1 + (\omega\tau)^z \sin\left(\frac{\alpha\pi}{2}\right)} \right\} \quad (11)$$

Combining eqn (9)–(11) with $\sigma'(\omega) \sim \omega \varepsilon''(\omega)$, as in eqn (7), the Debye term is modified ($\sigma'(\omega) \propto \omega^s$). Fig. 6(b) shows the fitting result with eqn (8) and with the distribution function including

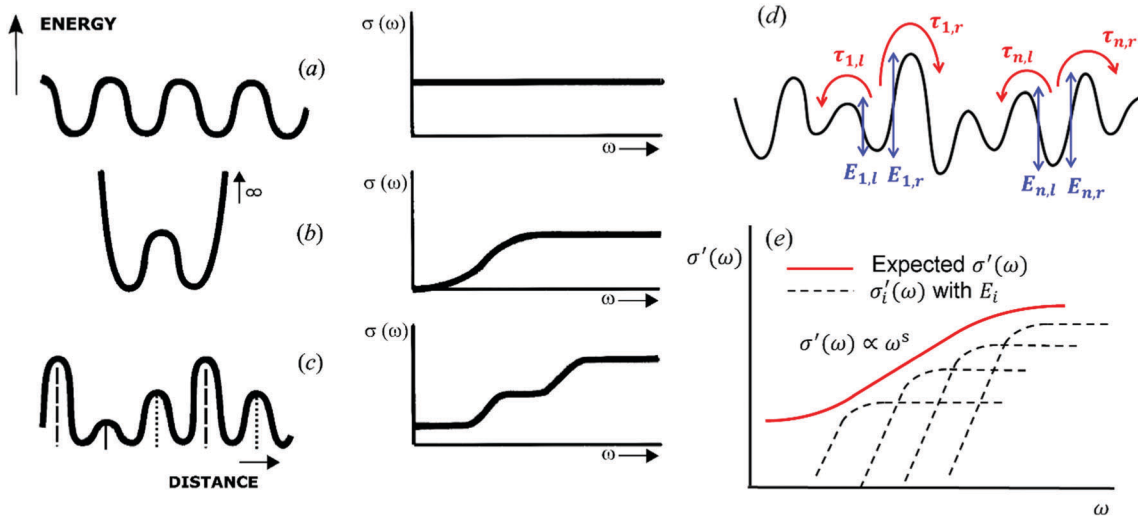


Fig. 5 Frequency dependence of the hopping conductivity for different potential energy profiles: (a) periodic constant activation energy, (b) a single bi-well, and (c) a potential profile with three different activation energies, modified and redrawn from ref. 21. (d) The distributed potential well proposed in this work, and (e) the expected conductivity profile with the potential energy profile of (d). Notations l and r in (d) represent the hopping direction and 1, i and n represent the lattice sites.

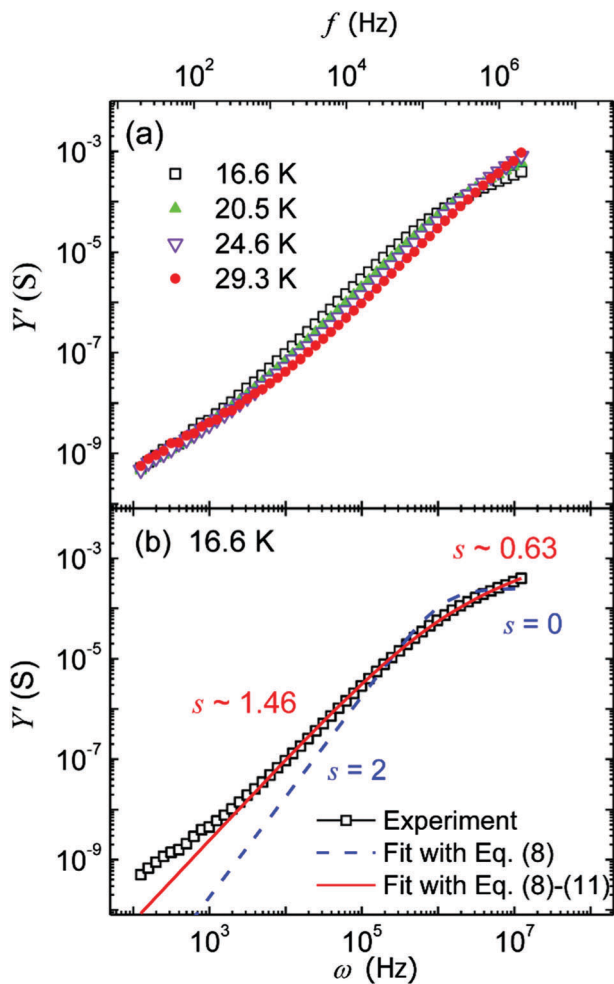


Fig. 6 (a) The a.c. conductance of n-NITO at different temperatures, and (b) the fitting result of the Debye model and the Havriliak-Negami (H-N) model.

eqn (9)–(11). The model modified by the distribution function fits very well with the experimental data for both sides of ω_r . This result proves that the $Y(\omega)$ value is affected by the distributed potentials in n-NITO at low temperatures.

In summary, dielectric spectroscopy and the H-N fitting predict the hopping electrons around the distributed localized states contributing to the CP. The distributed hopping model introduced here successfully explains both the broad peak in the dielectric loss and the frequency-dependent a.c. conductance. The results demonstrate that the observed two phenomena are correlated and support the proposed distributed hopping model.

Conclusions

We performed dielectric spectroscopy on a SPS n-NITO ceramic system. The electrode–ceramic interface effect was ruled out as the origin of the large permittivity. Huge dielectric relaxation was observed below 35 K. The H-N analysis suggested that the Debye-like relaxation had symmetric and distributed nature. The temperature dependence of the distribution was shown to

be weakly dependent on temperature. The fast relaxation process, owing to the small values of E_a and τ_0 , suggests that the relaxation is attributed to the hopping motion of electrons, which are believed to be localized at the cation site. The mean relaxation time was found to be much faster than that of dipolar reorientation or interfacial relaxation. The a.c. transport at this temperature range was successfully explained by the hopping conduction model with H-N parameters. The strong correlation between the relaxation and the a.c. conductance suggests that the large dielectric relaxation and broadened distribution should be associated with the hopping motion of localized electrons. A modified hopping model was introduced to account for this effect and should be applied to other systems involving localized hopping behavior.

Acknowledgements

This work is supported by the National Science Foundation, as part of the Center for Dielectrics and Piezoelectrics under Grant No. IIP-1361571 and 1361503. The authors would like to thank Mr Jeffery Long for electrical characterization, and Dr T. J. M. Bayer and Dr J. Bock for useful discussion. K. Tsuji would like to thank the ITO Foundation for International Education Exchange for financial support. The authors also thank the FERMAT federation for funding.

References

- 1 D. C. Sinclair, T. B. Adams, F. D. Morrison and A. R. West, *Appl. Phys. Lett.*, 2002, **80**, 2153–2155.
- 2 S. Krohns, P. Lunkenheimer, S. G. Ebbinghaus and A. Loidl, *Appl. Phys. Lett.*, 2007, **91**, 39–42.
- 3 J. Wu, C.-W. Nan, Y. Lin and Y. Deng, *Phys. Rev. Lett.*, 2002, **89**, 217601.
- 4 X. Kuang, C. Bridges, M. Allix, J. B. Claridge, H. Hughes and M. J. Rosseinsky, *Chem. Mater.*, 2006, **18**, 5130–5136.
- 5 S. Sarkar, P. K. Jana, B. K. Chaudhuri and H. Sakata, *Appl. Phys. Lett.*, 2006, **89**, 2004–2007.
- 6 S. Krohns, P. Lunkenheimer, C. Kant, A. V. Pronin, H. B. Brom, A. A. Nugroho, M. Diantoro and A. Loidl, *Appl. Phys. Lett.*, 2009, **94**, 1–4.
- 7 W. Hu, Y. Liu, R. L. Withers, T. J. Frankcombe, L. Norén, A. Snashall, M. Kitchin, P. Smith, B. Gong, H. Chen, J. Schiemer, F. Brink and J. Wong-Leung, *Nat. Mater.*, 2013, **12**, 821–826.
- 8 Z. Gai, Z. Cheng, X. Wang, L. Zhao, N. Yin, R. Abah, M. Zhao, F. Hong, Z. Yu and S. Dou, *J. Mater. Chem. C*, 2014, **2**, 6790.
- 9 X. Cheng, Z. Li and J. Wu, *J. Mater. Chem. A*, 2015, **3**, 5805–5810.
- 10 W. Tuichai, S. Danwittayakul, S. Maensiri and P. Thongbai, *RSC Adv.*, 2016, **6**, 5582–5589.
- 11 J. Li, F. Li, C. Li, G. Yang, Z. Xu and S. Zhang, *Sci. Rep.*, 2015, **5**, 8295.
- 12 Y. Q. Wu, X. Zhao, J. L. Zhang, W. B. Su and J. Liu, *Appl. Phys. Lett.*, 2015, **107**, 2–7.
- 13 Y. Song, X. Wang, Y. Sui, Z. Z. Liu, Y. Zhang, H. Zhan, B. Song, Z. Z. Liu, Z. Lv, L. Tao and J. Tang, *Sci. Rep.*, 2016, **6**, 21478.

- 14 S. Mandal, S. Pal, A. K. Kundu, K. S. R. Menon, A. Hazarika, M. Rioult and R. Belkhou, *Appl. Phys. Lett.*, 2016, **109**, 92906.
- 15 W. Dong, W. Hu, A. Berlie, K. Lau, H. Chen, R. L. Withers and Y. Liu, *ACS Appl. Mater. Interfaces*, 2015, **7**, 25321–25325.
- 16 H. Han, C. Davis and J. C. Nino, *J. Phys. Chem. C*, 2014, **118**, 9137–9142.
- 17 S. Sulekar, J. H. Kim, H. Han, P. Dufour, C. Tenailleau, J. C. Nino, E. Cordocillo, H. Beltran-Mir, S. Dupuis and S. Guillemet-Fritsch, *J. Mater. Sci.*, 2016, **51**, 7440–7450.
- 18 P. J. W. Debye, *Polar molecules*, Chemical Catalog Company, Incorporated, 1929.
- 19 S. Havriliak and S. Negami, *Polymer*, 1967, **8**, 161–210.
- 20 A. K. Jonscher, *Universal relaxation law: a sequel to Dielectric relaxation in solids*, Chelsea Dielectrics Press, 1996.
- 21 E. Barsoukov and E. J. Ross Macdonald, *Impedance spectroscopy: theory, experiment, and applications*, John Wiley & Sons, 2005.
- 22 H. Han, P. Dufour, S. Mhin, J. H. Ryu, C. Tenailleau and S. Guillemet-Fritsch, *Phys. Chem. Chem. Phys.*, 2015, **17**, 16864–16875.
- 23 M. Li, Z. Shen, M. Nygren, A. Feteira and D. C. Sinclair, *J. Appl. Phys.*, 2009, **106**, 104106.
- 24 J. Anthony and J. M. Herbert, *Electroceramics: materials, properties, applications*, John Wiley & Sons, 2003.
- 25 K. Tsuji, W.-T. Chen, H. Guo, X.-M. Chen, T.-K. Lee, W.-H. Lee and C. A. Randall, *RSC Adv.*, 2016, **6**, 92127–92133.
- 26 R. A. Maier and C. A. Randall, *J. Am. Ceram. Soc.*, 2016, **3359**, 3350–3359.
- 27 R. A. Maier and C. A. Randall, *J. Am. Ceram. Soc.*, 2016, **3366**, 3360–3366.
- 28 C. Wang, N. Zhang, Q. Li, Y. Yu, J. Zhang, Y. Li and H. Wang, *J. Am. Ceram. Soc.*, 2015, **98**, 148–153.
- 29 S. H. Cha and Y. H. Han, *Jpn. J. Appl. Phys.*, 2006, **45**, 7797–7800.
- 30 Z. Z. Wang, M. Cao, Q. Zhang, H. Hao, Z. Yao, Z. Z. Wang, Z. Song, Y. Zhang, W. Hu and H. Liu, *J. Am. Ceram. Soc.*, 2015, **98**, 476–482.
- 31 K. H. Lee and D. J. Eisenberg, *Phys. Lett. A*, 1980, **77**, 369–371.
- 32 M. Pollak and T. H. Geballe, *Phys. Rev.*, 1961, **122**, 1742–1753.
- 33 V. V. Lemanov, A. V. Sotnikov, E. P. Smirnova and M. Weihnacht, *J. Appl. Phys.*, 2005, **98**, 056102.
- 34 V. V. Lemanov, A. V. Sotnikov, E. P. Smirnova and M. Weihnacht, *Phys. Solid State*, 2002, **44**, 2039–2049.
- 35 C. C. Wang and L. W. Zhang, *New J. Phys.*, 2007, **9**, 0–10.
- 36 L. A. K. Dominik and R. K. MacCrone, *Phys. Rev.*, 1967, **163**, 756–768.
- 37 S. Komine and E. Iguchi, *J. Phys.: Condens. Matter*, 2004, **16**, 1061–1073.
- 38 R. Zorn, *J. Polym. Sci., Part B: Polym. Phys.*, 1999, **37**, 1043–1044.
- 39 E. Courtens, *Phys. Rev. Lett.*, 1984, **52**, 69–72.
- 40 J. R. Macdonald, *Ann. Biomed. Eng.*, 1992, **20**, 289–305.
- 41 L. A. Dominik and R. K. MacCrone, *Phys. Rev.*, 1967, **156**, 851–857.
- 42 M. Maglione and M. Belkaoumi, *Phys. Rev. B: Condens. Matter Mater. Phys.*, 1992, **45**, 2029–2034.
- 43 A. K. Jonscher, *J. Phys. D: Appl. Phys.*, 1999, **32**, R57–R70.
- 44 S. Saha and T. P. Sinha, *J. Phys.: Condens. Matter*, 2002, **14**, 249–258.
- 45 M. Pollak, *Phys. Rev.*, 1964, **133**, 564–579.
- 46 I. G. Austin and N. F. Mott, *Adv. Phys.*, 1969, **18**, 41–102.